Molecular Cell
Article

NELF Interacts with CBC and Participates in 3′ End Processing of Replication-Dependent Histone mRNAs

Takashi Narita,[1,5,6] Tetsu M.C. Yung,[1,5] Junichi Yamamoto,[1] Yasunori Tsuboi,[1,4] Hideyuki Tanabe,[2] Kiyoji Tanaka,[3] Yuki Yamaguchi,[1] and Hiroshi Handa[1,*]
[1] Graduate School of Bioscience and Biotechnology, Tokyo Institute of Technology, 4259 Nagatsuta, Yokohama, Kanagawa 226-8501, Japan
[2] Department of Biosystems Science, School of Advanced Sciences, The Graduate University for Advanced Studies (Sokendai), Shonan Village, Hayama, Kanagawa 240-0193, Japan
[3] Graduate School of Frontier Biosciences, Osaka University, Suita, Osaka 565-0871, Japan
[4] Aphoenix Inc., Tokyo 141-0021, Japan
[5] These authors contributed equally to this work.
[6] Present address: Graduate School of Frontier Biosciences, Osaka University, Suita, Osaka 565-0871, Japan.
*Correspondence: hhanda@bio.titech.ac.jp
DOI 10.1016/j.molcel.2007.04.011

SUMMARY

Negative elongation factor (NELF) is a four subunit transcription elongation factor that has been implicated in numerous diseases ranging from neurological disorders to cancer. Here we show that NELF interacts with the nuclear cap binding complex (CBC), a multifunctional factor that plays important roles in several mRNA processing steps, and the two factors together participate in the 3′ end processing of replication-dependent histone mRNAs, most likely through association with the histone stem-loop binding protein (SLBP). Strikingly, absence of NELF and CBC causes aberrant production of polyadenylated histone mRNAs. Moreover, NELF is physically associated with histone gene loci and forms distinct intranuclear foci that we call NELF bodies, which often overlap with Cajal bodies and cleavage bodies. Our results point to a surprising role of NELF in the 3′ end processing of histone mRNAs and also suggest that NELF is a new factor that coordinates different mRNA processing steps during transcription.

INTRODUCTION

Negative elongation factor (NELF) is a transcription factor composed of four subunits, NELF-A, -B, -C/D, and -E, of which certain subunits have been implicated in the etiology of various diseases. For example, NELF-A was found to be encoded by *WHSC2*, a candidate gene for a multiple malformation syndrome called the Wolf-Hirschhorn syndrome (Wright et al., 1999; Yamaguchi et al., 2001); NELF-B is a cofactor of BRCA1, an important breast/ovarian cancer susceptibility gene (Narita et al., 2003; Ye et al., 2001); and, finally, both NELF-B and NELF-E are found to be overexpressed in cancers of the upper digestive system (McChesney et al., 2006; Midorikawa et al., 2002).

NELF was originally found on the basis of its biochemical activity to suppress transcription elongation (Narita et al., 2003; Yamaguchi et al., 1999). NELF induces promoter-proximal pausing of RNA polymerase II (RNAPII) (Aida et al., 2006; Wu et al., 2003; Yamaguchi et al., 1999), in collaboration with DRB sensitivity-inducing factor (DSIF), which is then released following kinase P-TEFb-mediated hyperphosphorylation of the C-terminal domain (CTD) of RNAPII (Wada et al., 1998; Yamaguchi et al., 1999) and DSIF (Yamada et al., 2006). This negative regulation of NELF has been observed at different stages during transcription, which often depends on the target genes. For example, NELF is reported to keep the *hsp70* gene in a primed transcriptional state under normal conditions by binding to and inducing promoter-proximal pausing of RNAPII. Then, upon heat shock, this suppression is released, leading to rapid and high output of hsp70 proteins (Wu et al., 2003). In contrast to the *hsp* gene, NELF is shown to attenuate transcription levels by being recruited to estrogen-responsive genes following, rather than before, stimulation (Aiyar et al., 2004). Yet in other instances such as *junB* and other immediate-early genes, NELF attenuates transcription both before and after induction (Aida et al., 2006). Thus, it appears that NELF can function at various steps during transcription, although we still do not have sufficient information on how and why NELF functions at different steps during transcription.

NELF-induced transcription suppression has been proposed to provide a window of time for proper coordination of transcript processing (Aiyar et al., 2004; Fujinaga et al.,

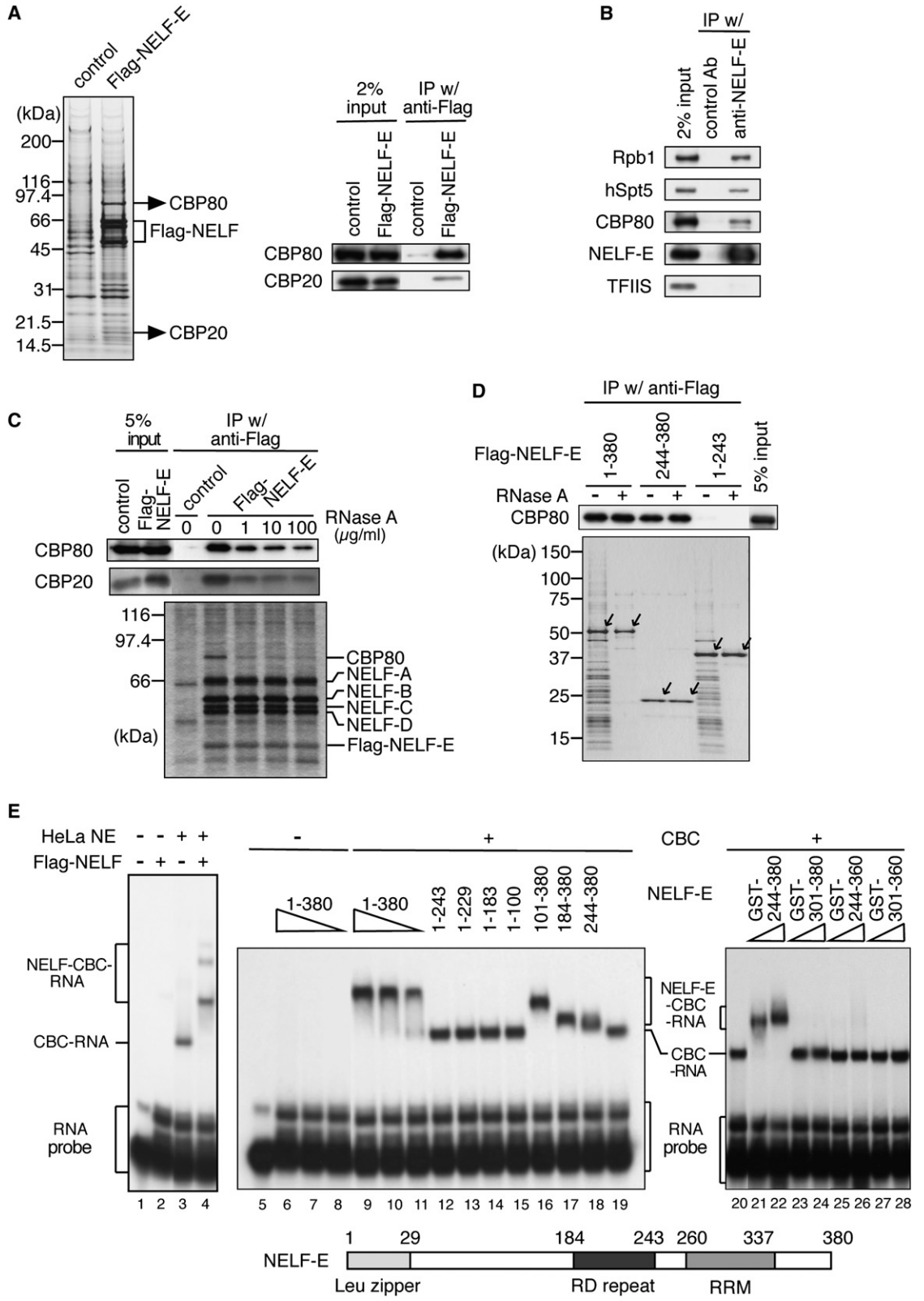

Figure 1. NELF Interacts with Nuclear Cap Binding Complex

(A) NE of wild-type HeLa cells (control) or HeLa cells stably expressing Flag-NELF-E were subjected to immunoprecipitation using anti-Flag antibody. The inputs and bound materials were analyzed by silver staining (left) or immunoblotting with the indicated antibodies (right).

2004; Wu et al., 2003) in what is referred to as elongation checkpoint control (Mandal et al., 2004; Pei et al., 2003). This is highly relevant to the emerging model of transcription regulation, which takes on an integrated view of mRNA processing steps; i.e., capping, splicing, and polyadenylation are now all thought to be interrelated and occur cotranscriptionally (Proudfoot et al., 2002) rather than independently of each other. Clearly, then, certain protein factors that play more than one role in different steps are likely to exist. The first and most obvious case of such a factor is RNAPII, and the effects of the presence or absence of the CTD, or its phosphorylation state, on capping, splicing, and polyadenylation have been well documented (Hirose and Manley [2000] and references therein). Another example of such a multifunctional factor is nuclear cap binding complex (CBC), which binds to the 5′ cap structure of maturing RNA and facilitates its export. It has been shown that, besides its functions in RNA export, CBC influences the rate of RNA backbone cleavage steps during splicing (Izaurralde et al., 1994) and also 3′ end processing (Flaherty et al., 1997; Proudfoot et al., 2002). Hence, these and other examples of multifunctional factors, such as cleavage and polyadenylation specificity factor (CPSF [Proudfoot et al., 2002]), support the integrated view of mRNA processing during transcription. However, it is still not possible to clearly illustrate this emerging model of transcription, as a minimal list of the key players involved have not yet been established.

Based on our previous report and our results presented here, we believe that NELF is one of these key factors. Recently, we have shown biochemically that NELF-mediated repression of transcription is released following the recruitment of capping enzyme to the elongation complex (Mandal et al., 2004), suggesting potential nuclear transactions between NELF and certain factors related to the mRNA 5′ cap. Here, in our initial search for cellular interactors of NELF, we found CBC as a major interactor of NELF. Strikingly, when either NELF or CBC was knocked down, a common but unique phenotype was observed, which was the accumulation of a polyadenylated form of the mRNAs of replication-dependent histones. This is highly unusual, as replication-dependent histone mRNAs, unlike replication-independent histone mRNAs and other general mRNAs, do not normally end in poly(A) tails (Marzluff, 2005), thus suggesting that NELF and CBC may function together in 3′ end processing of histone mRNAs. By using various biochemical and cell biological techniques, we have uncovered a physiological function of NELF in the maturation of replication-dependent histone mRNAs, which may be extended to the maturation of other types of RNAs, such as snRNAs. More importantly, our results suggest that NELF is a new factor that coordinates various mRNA processing steps during transcription and support the contemporary model of integrated transcription regulation.

RESULTS

NELF Interacts with Nuclear Cap Binding Complex

As very little is known about the physiological functions of NELF and other cellular factors that may be involved, in this investigation we first sought to identify proteins that interact with NELF in mammalian cells. NELF-interacting proteins were purified by immunoprecipitation with anti-Flag antibody from nuclear extracts (NE) prepared from HeLa cells that stably express Flag-tagged NELF-E (Flag-NELF-E). Under stringent conditions, functionally active NELF complex (Flag-NELF) can be purified using this procedure (Narita et al., 2003). Under milder binding and washing conditions, various extra proteins copurified specifically with Flag-NELF (Figure 1A). Such bands were excised from gels and subjected to mass spectrometric analyses, which revealed that several of the associated proteins were known NELF-interacting proteins, including RNAPII subunits (rpb1) and the hSpt5 subunit of DSIF (Yamaguchi et al., 1999). In addition, we identified CBP80 and CBP20, which are the two subunits of the CBC, as NELF-interacting proteins. The identity of CBP80 and CBP20 was confirmed by immunoblotting (Figure 1A). To confirm that endogenous NELF also interacts with CBC, immunoprecipitation was carried out with HeLa cell NE using control or anti-NELF-E antibodies, and the precipitates were analyzed as above. In addition to Rpb1 and hSpt5, CBP80 coprecipitated with NELF-E, while a control protein, TFIIS, did not (Figure 1B). These results suggest that NELF interacts with CBC in HeLa cells.

Since both NELF and CBC are RNA binding factors, we next examined whether or not RNA is involved in the interaction between NELF and CBC. Immunoprecipitation using anti-Flag antibody was carried out with HeLa/Flag-NELF-E cell NE pretreated with various concentrations of RNase A. Increasing amounts of RNase A resulted in decreasing amounts of coprecipitated CBC, while the amount of immunoprecipitated Flag-NELF remained

(B) HeLa cell NE were subjected to immunoprecipitation using anti-Flag (control Ab) or anti-NELF-E antibody. The input and bound materials were analyzed by immunoblotting with the indicated antibodies.
(C) Wild-type HeLa or HeLa/Flag-NELF-E NE were treated with the indicated concentrations of RNase A, followed by immunoprecipitation with anti-Flag antibody. The input and bound materials were analyzed by immunoblotting (top) or silver staining (bottom).
(D) Sf9 cells were coinfected with the recombinant baculoviruses that express CBP80, CBP20, and full-length (1–380) or truncated mutant Flag-NELF-E, as indicated. Immunoprecipitation was carried out on the cell lysates using anti-Flag antibody, and the precipitates were analyzed by immunoblotting (top) or Coomassie staining (bottom). Arrows indicate the expected sizes of full-length or mutant Flag-NELF-E.
(E) The indicated combinations of protein factors (HeLa NE, 0.2 μl [~1 μg protein]; Flag-NELF, 20 ng; NELF-E [1–380], 20, 40, and 60 ng; NELF-E mutants, 20 ng; GST-NELF-E mutants, 20 and 100 ng; CBC, 5 ng) were incubated with m^7GpppG capped RNA probe. Reactions were analyzed by electrophoresis on 4% native polyacrylamide gels. Also shown at the bottom is the structure of NELF-E. Leu zipper, leucine zipper; RD repeat, arginine/aspartic acid repeat; RRM, RNA recognition motif.

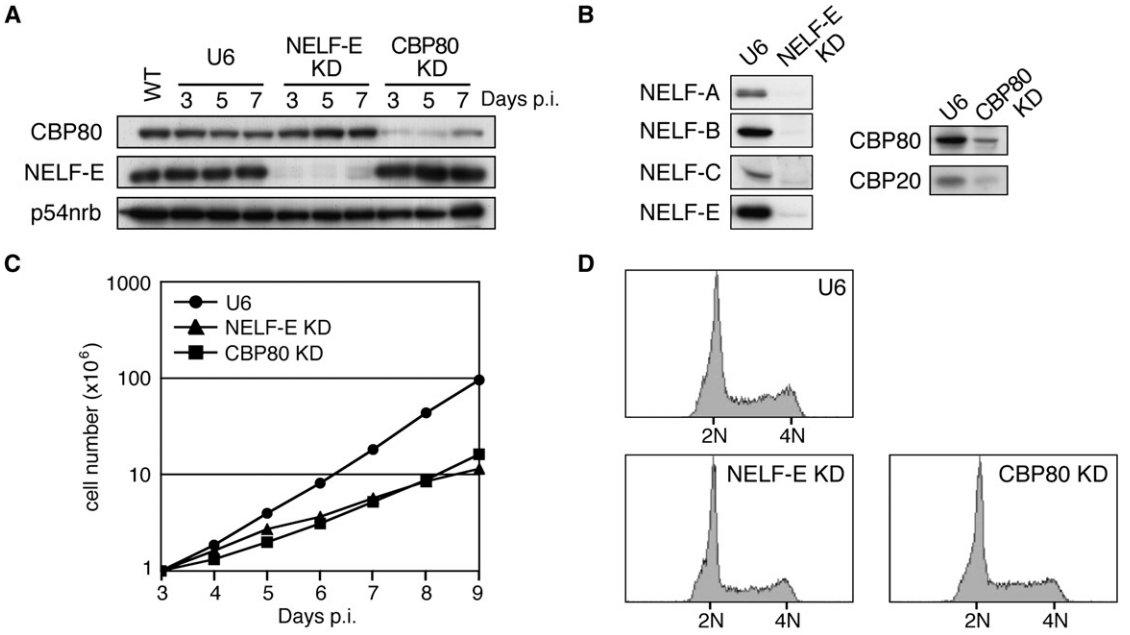

E

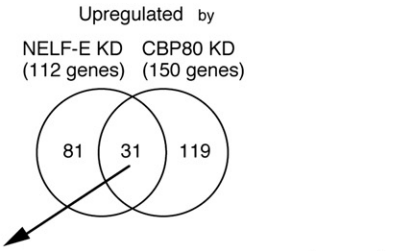

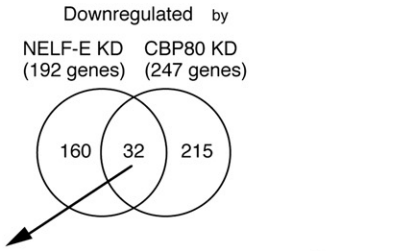

	Signal Log Ratio	
Gene symbol	NELF-E KD	CBP80 KD
CTGF	2.8	2.5
CYR61	1.3	1.1
DNAJB9	1.2	1.1
DUSP6	4.2	2.4
EPHA2	1.4	2.3
EPS8	1.4	1.4
ETV5	1.7	3.1
H2BFS	2.7	3.2
HIST1H1C	2.3	3.6
HIST1H2AC	1.5	2.8
HIST1H2AE	1.7	3.8
HIST1H2BD	1.7	2.8
HIST1H2BE	2.3	2.8
HIST1H2BF	1.7	3.0
HIST1H2BH	1.9	3.0
HIST1H2BI	1.6	2.8
HIST1H2BK	2.1	2.7
HIST1H3H	3.4	4.7
HIST2H2AA	3.8	3.7
JAG1	2.1	1.6
LAMA4	1.7	1.1
MAFF	1.2	1.9
NUP98	1.2	1.1
PHLDA1	2.3	2.3
PLK2	1.2	1.2
PRNP	1.2	1.3
RGS2	1.3	1.6
SERPINE2	2.5	2.2
SPOCK1	1.5	1.4
TPBG	1.5	1.6
VEGFC	1.1	1.3

	Signal Log Ratio	
Gene symbol	NELF-E KD	CBP80 KD
ACY1	-1.3	-2.2
AKT1	-1.2	-1.3
ALPI	-4.7	-3.6
ANXA6	-1.4	-1.5
ASS1	-4.3	-2.7
BTN3A3	-1.8	-3.9
C6orf48	-1.5	-1.4
CLNS1A	-1.2	-1.8
CLU	-1.6	-1.3
COL11A1	-1.3	-1.8
COPB2	-1.0	-1.0
CYBA	-1.3	-1.1
ENO3	-1.2	-1.1
FADS1	-1.0	-1.5
FSTL3	-1.3	-1.4
GPR56	-1.4	-1.7
HYAL1	-4.4	-2.2
IDH2	-1.2	-1.9
IMPA2	-2.4	-3.1
IMPDH2	-1.8	-1.9
KCNN2	-1.6	-1.3
KYNU	-1.2	-1.3
L1CAM	-3.5	-1.6
MCM5	-1.0	-1.2
MSRB2	-1.1	-2.8
PCCB	-1.1	-1.0
PIR	-1.1	-2.1
PRSS23	-1.9	-2.2
RRAS	-2.1	-1.4
TIMELESS	-1.3	-1.7
UCP2	-1.6	-1.3
WFDC1	-2.6	-1.1

constant (Figure 1C). However, even in the presence of high concentrations of RNase A, small amounts of CBC coimmunoprecipitated with Flag-NELF, indicating that there is at least a low-affinity direct interaction between NELF and CBC, which is expected to be highly stabilized by the presence of RNA.

Then, we determined which NELF subunit binds directly to CBC. For this purpose, each subunit of NELF, expressed as a GST fusion protein in *Escherichia coli*, was immobilized onto glutathione Sepharose beads and then incubated with CBP80 and CBP20 that were coexpressed by in vitro transcription and translation. Analysis of bound materials revealed that both CBP80 and CBP20 selectively bound to GST-NELF-E, but not to other GST fusion NELF subunits (see Figure S1A in the Supplemental Data available with this article online). These results suggest that NELF-E is the binding surface for CBC.

Next, we determined the NELF-E region required for CBC binding. Immunoprecipitation with anti-Flag antibody was carried out by using cell lysates prepared from insect Sf9 cells overexpressing CBP80 and CBP20 together with full-length or truncated versions of Flag-NELF-E, in the presence or absence of RNase A. As shown in Figure 1D, similar amounts of CBP80 coprecipitated with the short C-terminal fragment of Flag-NELF-E (amino acids 244–380) as with full-length Flag-NELF-E, while negligible amounts of CBP80 coprecipitated with the longer N-terminal fragment of Flag-NELF-E (amino acids 1–243). In this assay, RNase sensitivity was not observed, due most likely to the large amounts of recombinant NELF-E and CBC in this overexpression system, which supports the idea that NELF interacts directly with CBC. These results demonstrate that the short C-terminal sequence of NELF-E (amino acids 244–380) is involved in the interaction with CBC.

To further understand the interactions among NELF, CBC, and RNA, we carried out electrophoretic mobility shift assay (EMSA) with m^7GpppG-capped RNA, a high-affinity substrate for CBC (Figure 1E). When small amounts (0.2 μl) of HeLa NE were used as a source of CBC, a discrete slower-migrating band was observed (lane 3). An antibody against CBP80 caused a supershift of this band, indicating that the band corresponds to CBC-RNA complex (data not shown). When an amount of Flag-NELF (~20 ng) that did not by itself cause retardation of m^7GpppG-capped RNA probes (lane 2) was added to the reactions, much slower-migrating bands corresponding to NELF-CBC-RNA complexes appeared (lane 4). Several supershift bands were observed, probably because the Flag-NELF fractions used contained both intact Flag-NELF and NELF subassemblies (e.g., NELF-B/NELF-E subcomplex [Yamaguchi et al., 2002]). These results indicate that NELF binds preferentially to CBC-RNA complexes over RNA itself. Then N-terminally and C-terminally truncated versions of bacterially produced NELF-E were used in combination with purified recombinant CBC, which revealed, in agreement with the finding in Figure 1D, that the region from amino acids 244 to 380 of NELF-E containing an RNA-recognition motif is necessary and sufficient for the interaction between NELF and CBC-RNA complexes (Figure 1E, lanes 5–28). Importantly, deletion of the C-terminal 20 amino acids of NELF-E abolished its interaction with CBC-RNA complexes (lanes 20–28) but had negligible effect on its own RNA binding observed at a higher protein concentration (Figure S1B), as predicted from the primary structure of NELF-E. Together, these results lead us to conclude that the binding of NELF to CBC and RNA can be separated biochemically and that both of these interactions contribute to the formation of stable NELF-CBC-RNA complexes.

Knockdown of NELF-E and CBP80 Causes "Increased Expression" of Replication-Dependent Histone Genes

Given the tight association between NELF and CBC, it is plausible that they have common roles in vivo and that inhibition of the function of NELF and CBC could result in similar phenotypes. To address this issue, HeLa cells were transduced with lentiviral vectors expressing short hairpin (sh) RNAs against NELF-E and CBP80, which resulted in >90% knockdown of each target protein (Figure 2A). In addition, the protein levels of the other NELF subunits and CBP20 were also significantly reduced in cells that were knocked down in NELF-E and CBP80, respectively (Figure 2B). Since the mRNA levels of the other NELF subunits and CBP20 did not alter dramatically (Figure S2), these results suggest that free NELF subunits and CBP20 are unstable and degraded rapidly at the protein level and that knockdown of NELF-E and CBP80 abolishes the functional NELF holocomplex and CBC, respectively. As expected, both NELF-E and CBP80 knockdown cells exhibited a similar phenotype, which was a slower

Figure 2. Knockdown of NELF-E and CBP80 Causes "Increased Expression" of Replication-Dependent Histone Genes

(A) HeLa cells were transduced with lentiviral vectors not expressing shRNAs (U6) or expressing shRNAs against NELF-E or CBP80. Immunoblot analysis using anti-CBP80 or anti-NELF-E was carried out on the cell extracts at the indicated number of days postinfection (p.i.). p54nrb serves as a loading control.

(B) Immunoblotting using the indicated antibodies was carried out as in (A).

(C) Growth curve of NELF-E and CBP80 knockdown cells. HeLa cells were treated as described in (A) and then counted at the indicated number of days postinfection.

(D) Effect of NELF-E and CBP80 knockdown on cell-cycle distribution. At 5 days postinfection, the cell-cycle distribution was assessed by propidium iodide staining and fluorocytometric analysis.

(E) DNA microarray analysis in NELF-E and CBP80 knockdown cells. Genes that were upregulated or downregulated in both NELF-E and CBP80 knockdown cells are shown. The log scale of signal log ratio is base 2. Thus, a signal log ratio of 1.0 indicates an increase of the transcript level by 2-fold, and −1.0 indicates a decrease by half. Replication-dependent histone genes are boxed.

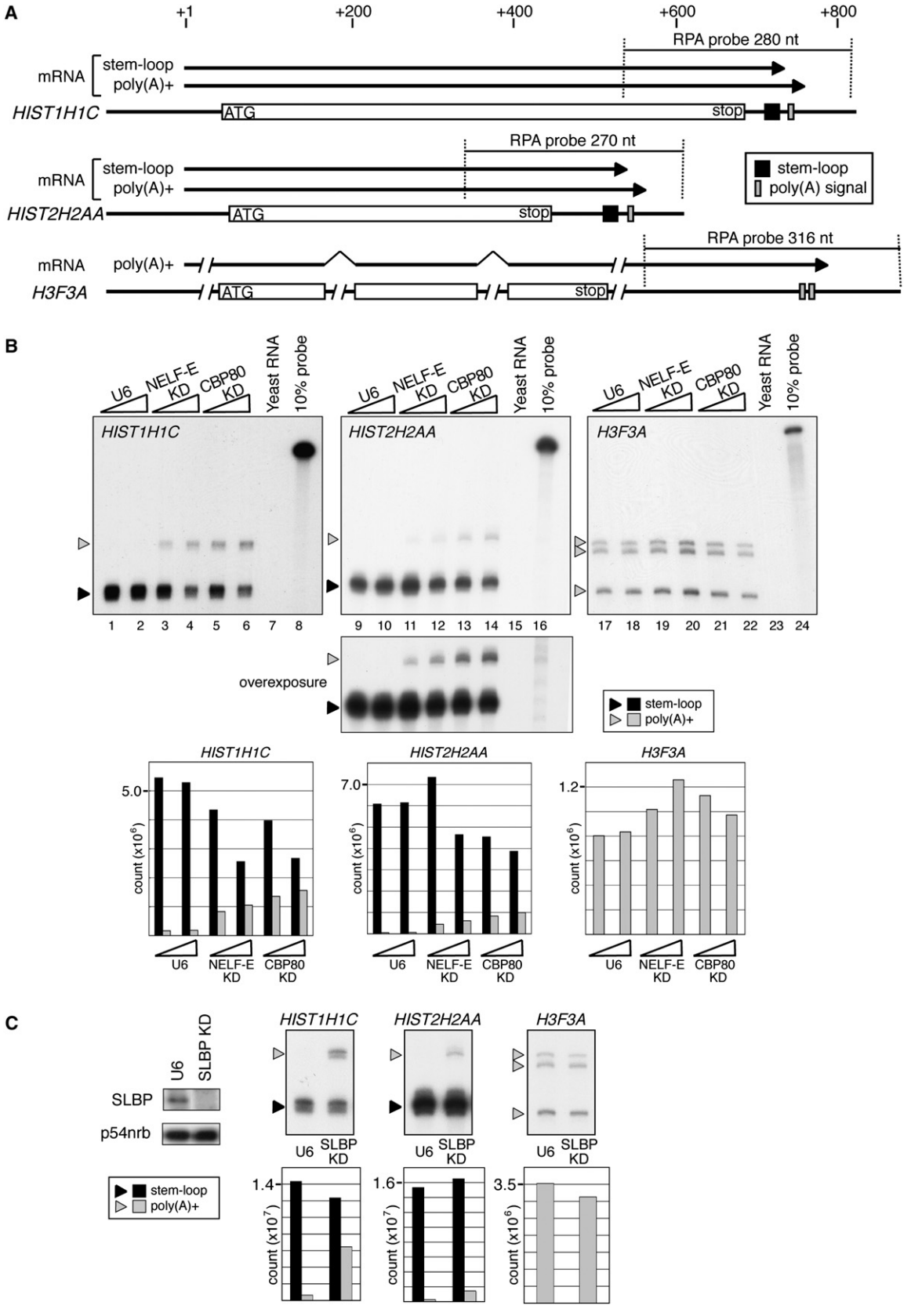
A
+1
+200
+400
+600
+800
RPA probe 280 nt
mRNA
stem-loop
poly(A)+
HIST1H1C
ATG
stop
RPA probe 270 nt
HIST2H2AA
stem-loop
poly(A) signal
RPA probe 316 nt
H3F3A
B
U6
NELF-E KD
CBP80 KD
Yeast RNA
10% probe
HIST1H1C
HIST2H2AA
H3F3A
1 2 3 4 5 6 7 8
9 10 11 12 13 14 15 16
17 18 19 20 21 22 23 24
overexposure
stem-loop
poly(A)+
count (x10^6)
5.0
7.0
1.2
C
U6
SLBP KD
SLBP
p54nrb
stem-loop
poly(A)+
count (x10^7)
1.4
1.6
count (x10^6)
3.5

growth rate relative to control HeLa cells (Figure 2C). This observation then prompted us to analyze the cell-cycle profiles of these cells by flow cytometry. Unexpectedly, there were no significant differences in cell-cycle distribution between control HeLa cells and cells knocked down in NELF-E or CBP80 (Figure 2D). Although the causes underlying this slow growth phenotype are presently unknown, the results nonetheless suggest that NELF and CBC functions are somehow linked to cell proliferation.

We then reasoned that gene expression profiles of factors related to cell proliferation may be altered in NELF and CBC knockdown cells. Therefore, we performed a DNA microarray analysis to explore gene expression changes in NELF-E and CBP80 knockdown cells. As shown in Figure 2E and Figure S2, we identified 112 genes and 150 genes that were specifically upregulated at least 2-fold (log ratio 1) in NELF-E and CBP80 knockdown cells, respectively. Similarly, 192 genes and 247 genes were downregulated at least 2-fold (log ratio −1) in NELF-E and CBP80 knockdown cells, respectively. We focused on the genes that were upregulated or downregulated in both NELF-E and CBP80 knockdown cells, with the objective of finding pathways in which both NELF and CBC may work together. The results showed that there are 31 upregulated genes and 32 downregulated genes that were common to both types of knockdown cells (Figure 2E). These results were further validated by quantitative RT-PCR analysis on three genes chosen arbitrarily from each group (Figure S3). Strikingly, of the 31 upregulated genes, 12 were replication-dependent histone genes, whereas no characteristic patterns or categories were discerned among the remaining genes in both lists. Normally, replication-dependent histone mRNAs are not polyadenylated but end instead in a conserved stem-loop structure. Hence, here, the fact that our microarray analysis, which only detects polyadenylated transcripts, showed "increased expression" of replication-dependent histone genes indicates that knocking down NELF-E or CBP80 causes aberrant production and accumulation of the polyadenylated form of these histone mRNAs in HeLa cells.

NELF and CBC Are, Similar to SLBP, Critical for 3′ End Processing of Replication-Dependent Histone Pre-mRNAs

Typical histone genes are intronless and have not only a conserved stem-loop structure but also a canonical polyadenylation signal downstream of the stem loop. This suggests that two kinds of transcripts, one that ends with the stem loop (stem-loop form) and the other that is slightly longer and has an additional poly(A) tail (poly(A)$^+$ form), can be generated. In fact, poly(A)$^+$ transcripts are found in the human EST database for a number of replication-dependent histone genes.

Here, we asked whether NELF and CBC affect the cellular decision in pursuing the stem-loop pathway or the polyadenylation pathway in 3′ end processing of histone pre-mRNAs by carrying out RNase protection assays using probes against two typical histone genes (*HIST1H1C* and *HIST2H2AA*) and one replication-independent histone gene (*H3F3A*), as depicted in Figure 3A. In control-transduced cells, only the stem-loop form of replication-dependent histone mRNAs was observed (Figure 3B, lanes 1, 2, 9, and 10), whereas in both NELF-E and CBP80 knockdown cells, polyadenylated transcripts were observed in addition to stem-loop form transcripts (lanes 3–6 and 11–14). On the other hand, the patterns and signal levels of the *H3F3A* mRNA bands did not change significantly following all three types of transductions (lanes 17–22). These results suggest that accumulation of poly(A)$^+$ histone mRNA can result from the absence of NELF or CBC function. As histone gene expression is tightly controlled during the cell cycle, one might argue that alterations in histone mRNA 3′ end processing in NELF-E and CBP80 knockdown cells may be an indirect result of the slow-growth phenotype (Figure 2C). However, this is unlikely because the knockdown had no discernable effect on the cell cycle (Figure 2D).

Mutations in SLBP, which is a central factor in histone mRNA 3′ end processing, cause the abnormal accumulation of polyadenylated replication-dependent histone mRNAs in flies (Lanzotti et al., 2002; Sullivan et al., 2001). As this phenotype highly resembles that of NELF-E and CBP80 knockdown cells, we needed to confirm that our observations here are the same as those reported for SLBP. Thus, SLBP was knocked down in HeLa cells (Figure 3C, left panels) with the same strategy as NELF-E and CBP80 knockdown, and the RNase protection assays as above were carried out by using RNA extracted from these cells. As expected, similar results were obtained with SLBP knockdown cells; i.e., accumulation of polyadenylated messengers for *HIST1H1C* and *HIST2H2AA* was observed, while negligible change was observed for *H3F3A* (Figure 3C).

Figure 3. NELF and CBC Are, Similar to SLBP, Critical for 3′ End Processing of Replication-Dependent Histone Pre-mRNAs

(A) Diagram of *HIST1H1C*, *HIST2H2AA*, and *H3F3A* genes and probes used for RNase protection assays. Open boxes represent open reading frames. Both stem-loop form and poly(A)$^+$ form transcripts are represented as arrows. The RPA probes are represented as bars.

(B) HeLa cells were transduced with recombinant lentiviruses, and total RNA was extracted at 5 days postinfection. Two micrograms of total RNA was analyzed by RNase protection assays with the indicated RNA probes. As a control, 2 μg of yeast RNA was treated under the same conditions with (Yeast RNA) or without (10% probe) RNase.

(C) (Left) HeLa cells were transduced with lentiviral vectors expressing shRNA against SLBP. At 5 days postinfection, cells were lysed and analyzed by immunoblotting. (Right) RNase protection assays were carried out as described in (B). (B and C) Gray and black arrowheads indicate poly(A)$^+$ form and stem-loop form transcripts, respectively. The counts of each transcript were quantified by using the image analyzer STORM (Molecular Dynamics). Note that several protected bands appeared in the case of *H3F3A*, most likely due to differential utilization of the poly(A) signals and to artificial cleavage of AU-rich sequences within the probe-target pair.

NELF and CBC Directly Affect 3′ End Processing of Histone Pre-mRNA

To ensure that the roles played by NELF and CBC in histone mRNA 3′ end processing were direct, we asked if the depletion of NELF or CBC would lead to the specific and aberrant accumulation of polyadenylated histone mRNAs even when the cryptic polyadenylation site was displaced upstream to the stem loop. To this end, we prepared mouse replication-dependent histone gene expression constructs containing an artificial 3′UTR region in which the stem-loop sequence and the polyadenylation signal were found either in the forward or reversed positions relative to each other (Figure 4A and Figure S4). Using this system, which contains both mouse (Figure 4B, first and second panels) and human (Figure 4B, third and fourth panels) stem-loop sequences and polyadenylation signals, we showed that, when these *cis* elements were cloned in the normal forward positions, an accumulation of the longer polyadenylated transcripts and a decreasing amount of the shorter normally processed transcripts took place when NELF-E or CBP80 was knocked down (first and third panels), consistent with earlier results (Figure 3B). Strikingly, when the positions of these *cis* elements were reversed, the accumulation of the now shorter polyadenylated transcripts and the decreasing amount of the now longer normally processed transcripts still occurred (Figure 4B, second and fourth panels), suggesting that the choice of the polyadenylation signal was a specific and direct result of the absence of NELF or CBC. As an additional control, we also showed that the knockdown of NELF or CBC resulted in marginal change in the levels of various factors involved in histone 3′ end processing, including SLBP, U7 snRNA, and Sm B/B′, an Sm core component of U7 snRNP and other U snRNPs (Figure S5). Consistent with our finding thus far, the knockdown of SLBP also led to similar results (Figure 4B and Figure S5). Taken together, we conclude that NELF and CBC play a critical and direct role in 3′ end processing of histone pre-mRNAs, which is likely related to SLBP functions.

CBC Interacts Directly with SLBP

To explore the possibility that NELF, CBC, and SLBP function within the same network of interacting proteins, we established a HeLa cell line constitutively expressing Flag-tagged SLBP (Flag-SLBP) and looked for SLBP-interacting proteins by employing anti-Flag affinity chromatography as in Figure 1. An ~80 kDa protein specifically copurified with Flag-SLBP (Figure 5A, lane 3) and was demonstrated to be CBP80 by immunoblot analysis (Figure 5A, lane 9). Further immunoblot analysis of the precipitates showed that CBP20 also clearly coimmunoprecipitated with Flag-SLBP (lane 9). In addition, since CBC coprecipitated with Flag-SLBP even in the presence of high RNase concentrations (Figure 5B), the interaction between CBC and SLBP is likely to be direct, similar to the interaction between CBC and NELF (Figure 1). Here, although coprecipitation of neither NELF-A nor NELF-E with SLBP was observed (Figure 5A, lane 9), a GST pull-down assay using GST-NELF-E with in vitro synthesized SLBP and CBP80/20 showed that GST-NELF-E was in fact able to pull down CBP80/20 and SLBP, but not an irrelevant protein luciferase (Figure 5C). Since more CBP80 was obtained regardless of whether we use NELF-E or SLBP as bait in coprecipitation assays, our results indicate that CBC is sandwiched between NELF and SLBP, which suggests that NELF plays its role in histone mRNA maturation by being brought into proximity of SLBP through an interaction with CBC.

NELF Accumulates in Nuclear Foci that Associate with Histone Loci, Cajal Bodies, and Cleavage Bodies

If NELF is indeed critical to histone mRNA 3′ end processing, then NELF should be located in areas where histone transcription and pre-mRNA processing occur in the cell. Of particular relevance to our work, it has been shown previously by a combined immunofluorescence (IF)/fluorescence in situ hybridization (FISH) method that a major cluster of histone genes found on the short arm of chromosome 6 is often associated with Cajal bodies (CB) (Frey and Matera, 1995), which are small discrete nuclear foci that contain its marker protein coilin, various transcription factors, splicing factors, and, importantly, histone mRNA maturation factors (Marzluff, 2005; Matera, 1999). Thus, we reasoned that a similar approach could allow us to study the relationships among NELF, histone loci, and CBs by obtaining their temporal-spatial data simultaneously in cells.

Here, we used probes against the same histone cluster on chromosome 6 as Frey and Matera (1995). The probes were first controlled for their specificity by FISH on a standard metaphase spread. As shown in Figure S6, the probe against the histone gene cluster and a chromosome painting probe against the short arm of chromosome 6 gave three overlapping signals in both the metaphase spread and in the interphase cell nucleus, demonstrating that our probe is specific against the histone gene cluster found on chromosome 6. The observation also indicates that the HeLa cells used here are aneuploid and that there are three copies of chromosome 6 in each cell, which is consistent with a previous report on the HeLa cell karyotype (Macville et al., 1999).

Next, this probe was employed to carry out a triple localization experiment, in which the localization of NELF was determined by expression of NELF-A tagged with enhanced yellow fluorescent protein (NELF-A-EYFP), histone loci by 3D FISH (Tanabe et al., 2005; Tanabe et al., 2002), and CBs by IF using an antibody against coilin. NELF-A-EYFP was localized in the nucleus (Figures 6A and 6D) as expected, but, significantly, was also accumulated in discrete intranuclear foci (Figure 6A, arrows) that often colocalized with histone loci and CBs (Figures 6B, 6C, and 6E). These intranuclear accumulations of NELF, the presence of which was also verified by IF using antibodies against each NELF subunit (data not shown), are

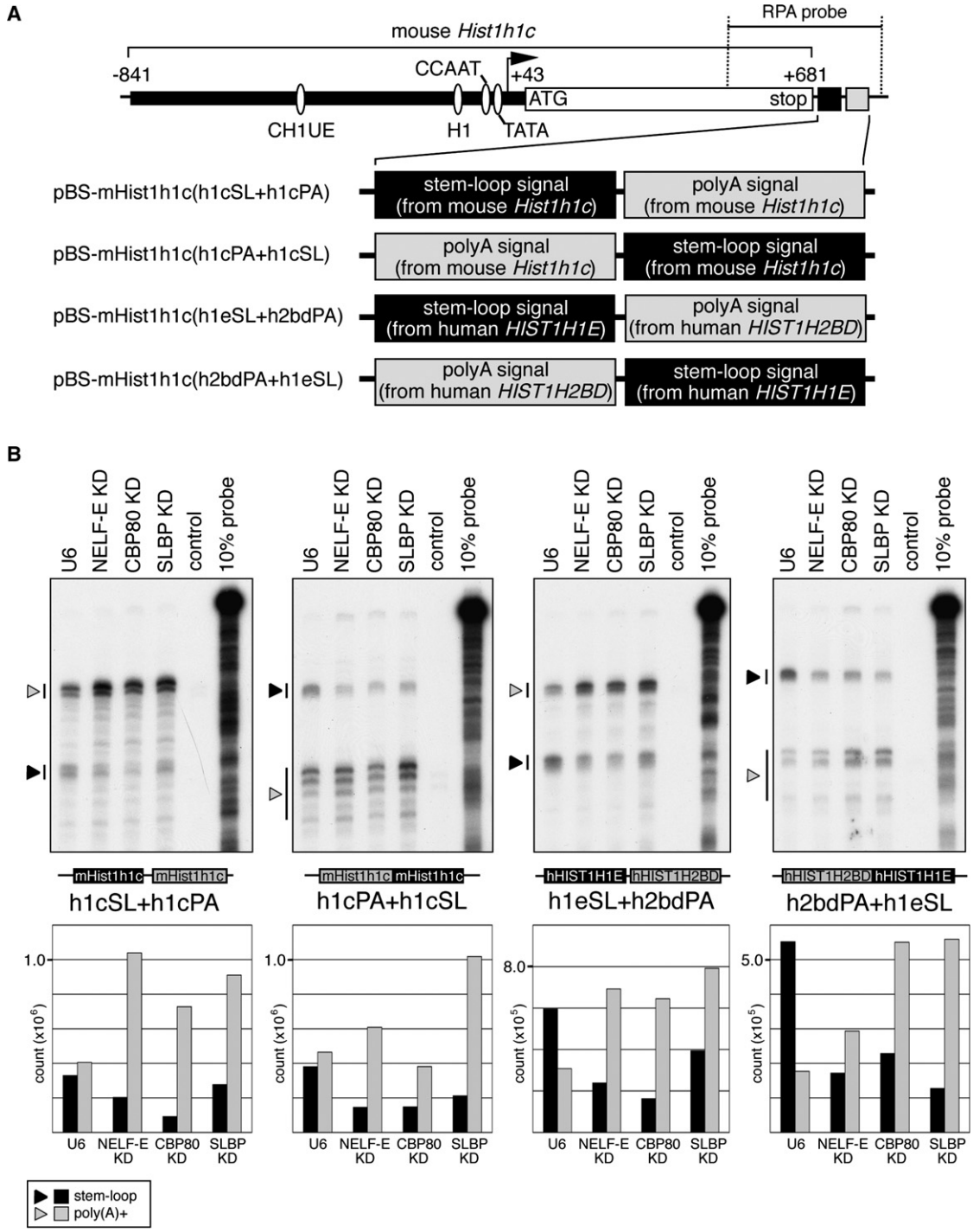

Figure 4. NELF and CBC Directly Affect 3′ End Processing of Histone Pre-mRNA

(A) Diagram of mouse *Hist1h1c* gene-based reporter constructs. Each reporter has, in addition to the *Hist1h1c* promoter and its entire coding region, a stem loop and a poly(A) signal from mouse or human histone genes, either in a forward or reversed order. Detailed sequences are shown in Figure S4. The transcription start site (+1) is indicated by the arrow. The open box represents the open reading frame of *Hist1h1c* gene. The four ellipses represent conserved sequence elements: CH1UE, H1 box, CCAAT box, and TATA box. The RPA probe is represented by a bar.

(B) The reporter plasmids were transfected into control or knockdown cells at 4 days postinfection. Total RNA was extracted at 2 days posttransfection, and 3 μg of the RNA was analyzed by RNase protection assays. As a control, 3 μg of total RNA prepared from control-transduced cells that were transfected with a control pBluescript plasmid was treated under the same conditions with (control) or without (10% probe) RNase. The notations and the quantification of each transcript are described in the legends for Figures 3B and 3C.

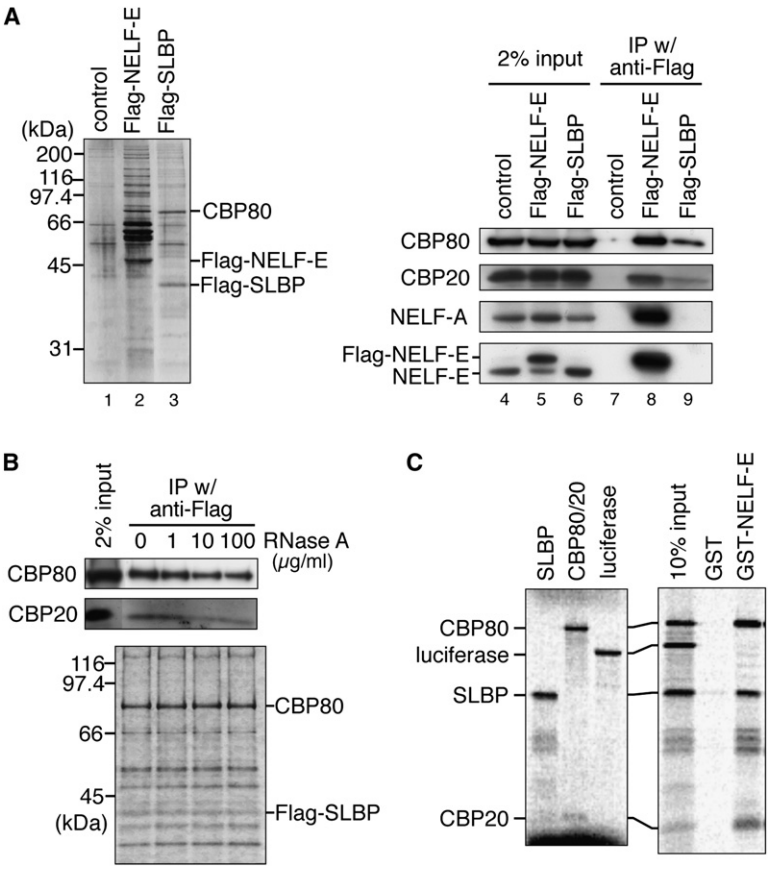

Figure 5. CBC Interacts Directly with SLBP

(A) NE from wild-type HeLa (control), HeLa/Flag-NELF-E, and HeLa/Flag-SLBP cells were subjected to immunoprecipitation with anti-Flag antibody. The inputs and bound materials were analyzed by silver staining (left) or immunoblotting with the indicated antibodies (right).

(B) HeLa/Flag-SLBP NE were treated with the indicated concentrations of RNase A, followed by immunoprecipitation with anti-Flag antibody. The input and bound materials were analyzed by immunoblotting (top) or silver staining (bottom).

(C) SLBP, CBP80/20, and luciferase proteins were synthesized and ^{35}S-labeled in vitro, and GST pull-down assays were carried out using a mixture of these in vitro-translated proteins and GST-NELF-E or GST. The inputs and bound materials were resolved by SDS-PAGE and analyzed by autoradiography.

often much smaller than CBs and number between one and four. Since NELF foci differed both in size and number from CBs, which are on average 0.2–2 μm and number between one and ten per cell (Cioce and Lamond, 2005; Frey and Matera, 1995), we will consider that these foci are distinct from CBs and will name them NELF bodies (NB). Intriguingly, the association rate between NBs and histone loci varied from cell to cell. We found that, of more than 150 NBs counted in cells synchronized either in early G1 or in S phase, the ratio between NBs associated with histone loci to those not associated during S phase was more than twice the same ratio in G1 phase (Figure 6F, middle). Furthermore, of the NBs that associated with histone loci, more than 90% were also associated with CBs. These results suggest that NELF plays a role in histone mRNA maturation by associating with histone genes, more in S phase when histone transcription is high than in early G1 phase, and CBs.

Interestingly, we noticed that NB/CB pairs often did not overlap perfectly. For example, the red arrow in Figure 6A points to a NB that is not aligned with its associated CB (i.e., no NELF-A-EYFP signal was detected in the center of the associated CB). In this respect, we note that the candidate histone 3′ cleavage factor CPSF (Dominski et al., 2005) has been reported to be concentrated in another type of intranuclear foci called cleavage bodies. NB and cleavage bodies are similar in that they are often smaller in size and fewer in number than CBs (Schul et al., 1996), but they differ in that cleavage bodies are predominantly found in S phase and G2 phase only (Li et al., 2006). Importantly, it is known that cleavage bodies are often found adjacent to, rather than completely overlapping with, CBs during S phase (Li et al., 2006; Schul et al., 1999). Based on these observations, we propose that NELF may first play a (possibly histone-related) role in CBs during G1 phase, after which NELF is transferred to associated histone genes/cleavage bodies where histone gene transcription and processing occur in S phase. In this context, then, it would be expected that NB/CB pairs that are associated with histone loci will be more aligned during early G1 phase and tend to be more misaligned during S phase, which is exactly what we found (Figure 6F, bottom). In support of our idea, IF staining of NELF-A-EYFP cells using an antibody against CstF64, a cleavage stimulation factor that is often used as a marker for cleavage bodies, shows that, of 13 NB/cleavage body pairs counted, all were quasi perfectly aligned (Figures 6G–6J and data not shown). As the presence per se of prominent cleavage bodies is indicative of cells in S phase, these data suggest that NELF functions in S phase are linked to cleavage bodies. Together, our fluorescence data suggest that NELF functions in histone mRNA maturation by

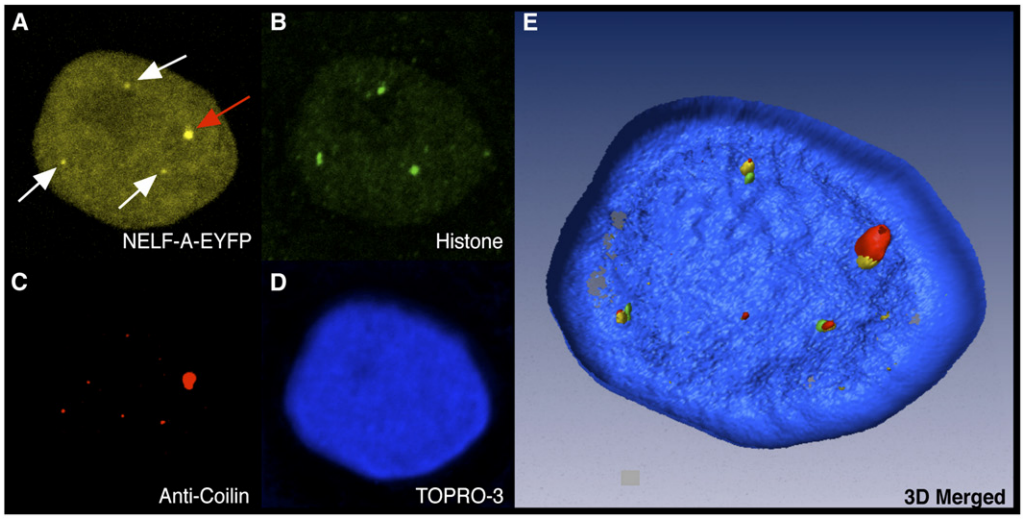

F

	Asynchronous	G1 Phase	S Phase
Total Cell Count	53	46	49
NB	157	155	190
(NB Associated with Hist): (NB Not Associated wth Hist)	(90):(67)	(80):(75)	(133):(57)
Ratio	1.34	1.07	2.33
NB Associated with Hist and CB	82	79	120
(NB Aligned with CB): (NB Not Aligned with CB)	(70):(12)	(69):(10)	(92):(28)
Ratio	5.83	6.90	3.28

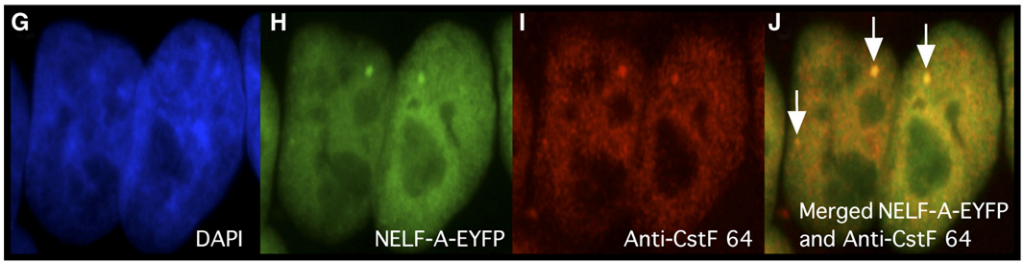

Figure 6. NELF Accumulates in Nuclear Foci that Associate with Histone Loci, Cajal Bodies, and Cleavage Bodies

(A–F) 3D-FISH combined with IF staining was performed on a HeLa cell line constitutively expressing NELF-A-EYFP (A), with DNA probes against a major histone gene cluster at 6p21.3 (B) and anti-coilin antibody (C), as described in the Experimental Procedures. DNA counterstained with TOPRO-3 is shown in blue (D). Each image shows a projection of a confocal series of optical sections through the scanned nucleus. The 3D merged image shows NELF bodies (yellow), histone loci (green), and Cajal bodies (red) simultaneously in one nucleus (E). Arrows point to NELF bodies associated (white) and not associated (red) with histone loci (A). (F) NELF bodies (NB), histone loci (Hist), and Cajal bodies (CB) were counted in asynchronous cells or cells synchronized either in G1 or S phase. Compiled data show the association between NELF bodies and histone gene loci and the alignment between Hist-associated NBs and CBs. "Alignment" is defined as "signal of NELF-A-EYFP detected in the center of the associated CB." (G–J) Fluorescence images of immunostaining carried out on NELF-A-EYFP-expressing HeLa cells using anti-CstF64 antibody are shown. Cells were stained with DAPI prior to image capture by standard fluorescence microscopy. Arrows point to NB/cleavage body pairs, which completely overlap.

associating with histone gene loci, CBs, and cleavage bodies in a temporal-spatially coordinated manner.

NELF and CBC Physically Associate with Histone Gene Loci

Finally, we carried out chromatin immunoprecipitation (ChIP) analysis to demonstrate the association between NELF and histone genes at the molecular level. In addition, as our IF analysis showed that CBC did not accumulate in any particular subnuclear domain (data not shown), we also carried out the same ChIP analysis targeting CBC in order to reinforce our idea that NELF's role in histone mRNA 3′ end processing is closely linked to that of CBC.

The first ChIP analysis was designed to verify the association of target proteins at the 5′ or 3′ end of one of the typical replication-dependent histone genes (*HIST1H1C*) used in our RNase protection assays (Figure 7A). As RNAPII likely serves as a platform for NELF and CBC to associate with histone loci, we first carried out the ChIP analysis using an antibody against Rpb1, the largest subunit of RNAPII. The results showed that RNAPII was found in both the 5′ and 3′ regions of *HIST1H1C*, but not in an irrelevant intergenic region on chromosome 2 (Figure 7B, RNAPII). Next, ChIP analysis using anti-Flag antibody was carried out using HeLa cells that stably express Flag-NELF-E or Flag-CBP20. As shown in Figure 7C, strong amplification signals were again detected in both the 5′ and 3′ regions of *HIST1H1C* for both Flag-NELF-E and Flag-CBP20, suggesting that NELF and CBC are found in both of these regions of replication-dependent histone genes in vivo. Since *HIST1H1C* is a relatively short gene, to ensure that our ChIP analysis had sufficient resolution to differentiate between the binding of factors at the 5′ versus the 3′ end of *HIST1H1C* and to rule out potential gene looping effects, ChIP analysis was carried out using anti-TBP, which yielded much stronger amplification signals for the 5′ end of *HIST1H1C* than the 3′ end, as is expected of a promoter binding protein (Figure 7B). In addition, another set of similar analyses was carried out on two other RNAPII-transcribed genes, *GAPDH* and the replication-independent histone gene *H3F3A* (Figures 7D–7F). Here, the results showed that comparatively little RNAPII, NELF, and CBC were found at the 3′ end relative to the 5′ end of these normally polyadenylated genes. Even at +700 of *H3F3A* and *GAPDH*, which is almost equivalent to the full length of *HIST1H1C*, only a relatively low amount of each protein was found, suggesting that the length of the gene is not a critical factor. Together, these results indicate that NELF and CBC are physically present in both the 5′ and 3′ regions of replication-dependent histone genes. In addition, the relatively higher amount of RNAPII at the 3′ region may reflect the presence of a rate-limiting step in transcription or processing.

DISCUSSION

In this study, we have shown that NELF plays an important role in the 3′ end processing of replication-dependent histone mRNAs in collaboration with CBC and SLBP. Although there is increasing acceptance of a transcription model in which the 3′ end processing of general mRNAs occurs cotranscriptionally and is integrated with other mRNA processing events, whether a similar mechanism exists for the 3′ end processing of replication-dependent histone mRNAs is still unknown. As NELF is a general transcription elongation regulator and CBC is known to play important roles in various transcription processing events, our results here provide evidence that the 3′ end processing of replication-dependent histone mRNAs likely also occurs cotranscriptionally and support the contemporary model that mRNA processing steps are integrated.

Histone Gene Expression and the Connection to Cajal Bodies and Cleavage Bodies

The expression level of replication-dependent histones is tightly regulated throughout the cell cycle and peaks at the beginning of S phase, where it can reach 35 times the level compared to other cell-cycle phases (Marzluff, 2005). Histone mRNAs are unique in that they are the only known metazoan mRNAs that are not polyadenylated, ending instead in a conserved stem-loop structure. Proper histone expression is dependent upon stoichiometric binding to this stem loop by SLBP, whose cell-cycle-dependent expression pattern mirrors that of histones. This binding apparently allows SLBP to stabilize the downstream binding of U7 snRNP, the histone-specific U snRNP, to its binding site called the histone downstream element (HDE). Although the distance between the stem loop and the HDE varies somewhat from gene to gene, the actual cleavage reaction invariably occurs upstream to the HDE (Scharl and Steitz, 1994, 1996). The stability of the U7 snRNP/HDE association is in turn highly critical for correct histone mRNA 3′ end cleavage, which most likely is carried out by CPSF (Dominski et al., 2005), the same cleavage factor for other nonhistone mRNAs.

Like their mRNAs, replication-dependent histone genes are also different from most other protein-encoding DNA sequences in that they are intronless and are linked in large clusters, mostly on the short arm of chromosome 6 and on the long arm of chromosome 1. Another characteristic feature of these histone gene loci is that they are known to be frequently associated with CBs (Frey and Matera, 1995), whose functions have been unclear for many years. In relation to our work, CBs have been proposed to play important roles in histone mRNA maturation, based on the fact that many of the required factors are found either within CBs themselves, e.g., RNAPII and various transcription factors, U7 snRNP, and SLBP, or in close proximity within associated bodies called cleavage bodies, e.g., CPSF (Marzluff, 2005; Schul et al., 1996).

Our results here show that NELF is also concentrated in distinct nuclear foci, NBs, associated with CBs and cleavage bodies (Figure 6), and that NELF is physically found on replication-dependent histone genes (Figure 7). However, how NELF makes its way into CBs, cleavage bodies, and

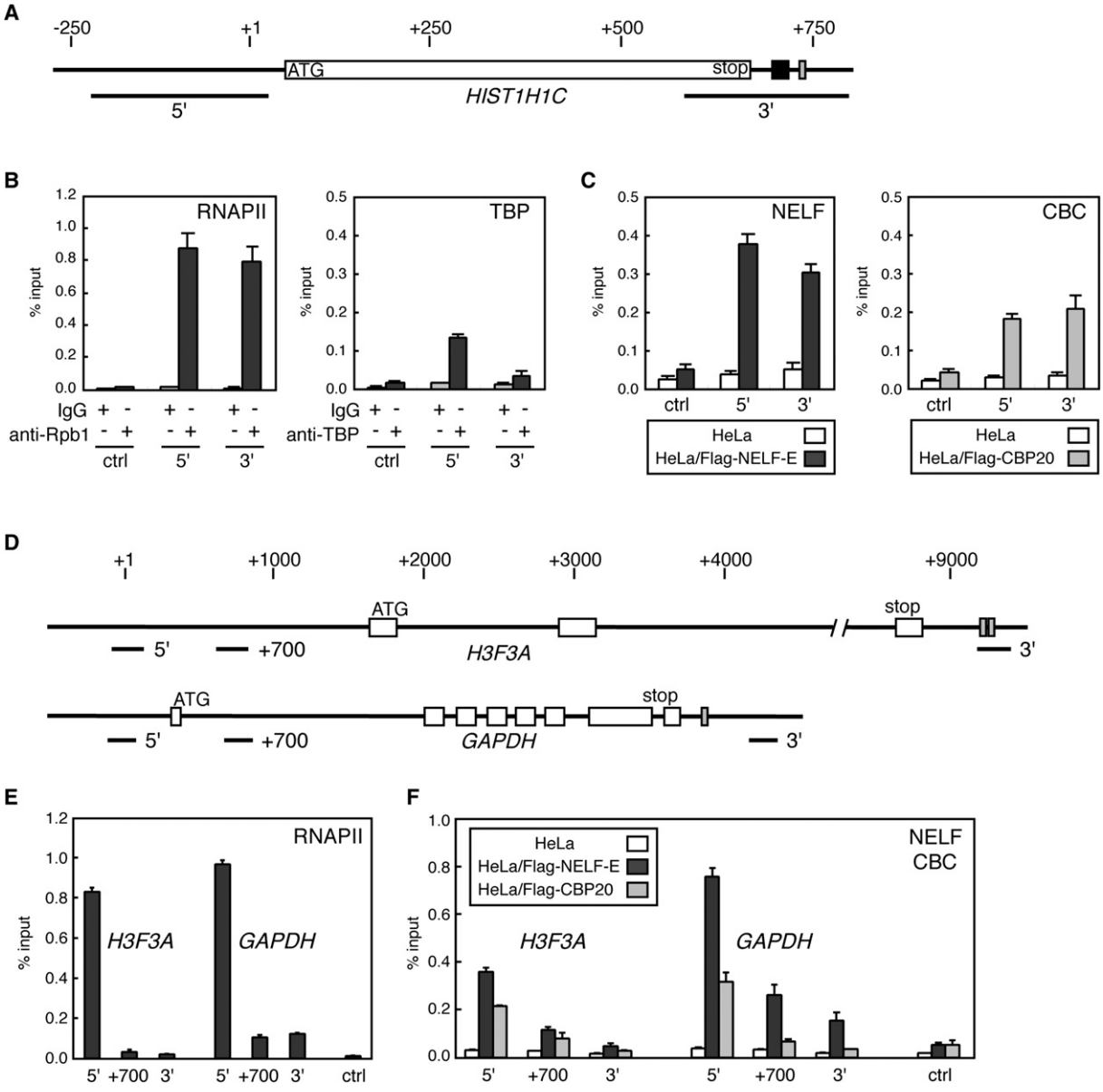

Figure 7. NELF and CBC Physically Associate with Histone Gene Loci

(A) Diagram of *HIST1H1C* gene. The notations are described in the legends for Figure 3A. The two amplicons (5′ and 3′) used for ChIP analysis are presented as bars under the diagram.

(B) Soluble chromatin from wild-type HeLa cells was subjected to ChIP analysis with control IgG, anti-Rpb1, or anti-TBP antibody. Real-time PCR was carried out using primers against a control intergenic region on chromosome 2 (ctrl) and against the 5′ and 3′ regions of *HIST1H1C*. Error bars represent the mean ±SEM from three independent experiments.

(C) ChIP analysis was performed as in (B) using anti-Flag antibody and control wild-type HeLa cells or HeLa cells that stably express Flag-NELF-E or Flag-CBP20. Error bars represent the mean ±SEM from three independent experiments.

(D) Diagram of *H3F3A* and *GAPDH* genes. The notations are described in the legends for Figure 3A. The six amplicons (5′, 3′, +700 for *H3F3A* and *GAPDH*) used for ChIP analysis are presented as bars under the respective diagrams.

(E) ChIP analysis was performed as in (B) using anti-Rpb1. Error bars represent the mean ±SEM from three independent experiments.

(F) ChIP analysis was performed as in (C). Error bars represent the mean ±SEM from three independent experiments.

near histone genes is not clear. The most straightforward explanation is simply by binding to RNAPII, which is highly concentrated in CBs, as mentioned above. Consistent with this idea is the fact that the state of CTD phosphorylation of the RNAPII concentrated in CBs is mainly in the form that has high affinity for NELF during RNAPII promoter-proximal pausing, i.e., phosphorylated on Ser-5 but not on Ser-2 (Gall, 2001; Xie and Pombo, 2006;

Yamaguchi et al., 1999). Interestingly, we also found that NBs often did not align with CBs during S phase (Figure 6F) but overlapped completely with cleavage bodies (Figures 6G–6J). As NBs are found throughout the cell cycle except during mitosis, whereas cleavage bodies are found predominantly during S phase and G2 phase (Li et al., 2006; Schul et al., 1996), NELF can be considered an early marker of subnuclear regions into which cleavage body components are assembled.

Role of NELF in Histone mRNA Maturation

What, then, are the actual functions of NELF in the maturation of replication-dependent histone mRNA at these specific intranuclear locations? Our previous report, which shows release of NELF-induced elongation repression following the recruitment of capping enzyme (Mandal et al., 2004), and probably also CBC, and our present coimmunoprecipitation data, which show that CBC is sandwiched between NELF and SLBP (Figure 5), suggest that the order of recruitment of the said factors to the mRNA is first NELF, then CBC, and finally SLBP. In this context, the key function of NELF may be to ultimately bring SLBP to its sites of action through an interaction with CBC. As absence of SLBP was previously shown to cause abnormal histone mRNA 3′ end processing (Sullivan et al., 2001), it is consistent, then, that cells knocked down in upstream factors NELF or CBC also exhibit similar phenotypes, as we have shown here (Figures 2–4). However, it was intriguing to us that, despite extensive knockdown of each of the factors, the endogenous level of polyadenylated replication-dependent histone messengers never exceeded that of normally processed messengers (Figure 3). One explanation, although only speculative, may be that certain factors do not have to be present at high levels for proper histone 3′ end processing. Hence it is plausible that, despite a low level of expression caused by the knockdown, the factors may still be able to carry out a major portion of the histone 3′ end processing, especially if it is considered as a priority function for the cell. In support of this idea, U7 snRNP, which is essential to histone 3′ end processing, is only present at a few hundred molecules per mammalian cell (Marzluff, 2005). NELF, on the other hand, is present in the order of 10^6 complexes per cell (data not shown).

Even though NELF plays its roles a few steps upstream to the actual cleavage reaction, our results suggest that NELF, by acting as a recruiter of CBC and SLBP, can greatly influence the decision between the stem-loop pathway and the polyadenylation pathway in histone mRNA 3′ end processing. Here, knockdown of NELF, CBC, or SLBP all resulted in the accumulation of longer polyadenylated histone mRNA (Figure 3) because a cleavage reaction that normally occurs upstream of the U7 snRNP/HDE RNA duplex (Scharl and Steitz, 1994, 1996) only took place after RNAPII encountered a polyadenylation signal further downstream. As SLBP-dependent cleavage and AAUAAA-dependent cleavage are probably both carried out by the same endonuclease CPSF (Dominski et al., 2005; Gilmartin, 2005), then the decisive element for proper histone mRNA 3′ end processing becomes the choice of the cleavage site. Here one may argue that, in agreement with the previously proposed elongation checkpoint control mechanism (Mandal et al., 2004; Pei et al., 2003), the slowing down of transcription elongation by NELF favors the selection of a more proximal, and hence the correct, cleavage site. However, while this assumption from the thermodynamic perspective is likely valid, it cannot explain how the depletion of NELF leads to the accumulation of polyadenylated histone mRNAs even when the polyadenylation sequence was moved upstream to the stem loop (Figure 4). Thus, although the exact mechanism remains to be elucidated, our results suggest that NELF is directly involved in the correct choice of the cleavage site in the stem-loop pathway and that, without NELF, the polyadenylation pathway is engaged by default.

Other Potential Roles of NELF in Coordinating RNA Maturation Steps

The fact that NELF is a multiple subunit complex, has high affinity for various types of RNA through the RRM domain of the subunit E (Yamaguchi et al., 2002), is tightly associated with cleavage bodies, and acts not only in the promoter-proximal region of RNAs but also at the 3′ end suggests that NELF likely plays many roles in different transcriptional processes. Incidentally, CBC, the strong NELF-interacting factor identified in this study, has been shown to enhance splicing reactions (Izaurralde et al., 1994), facilitate proper 3′ cleavage prior to polyadenylation (Flaherty et al., 1997), and stimulate transcript export (Izaurralde et al., 1995; Proudfoot et al., 2002). Considering the strong association between NELF and CBC and that they both work at the 5′ and 3′ ends of mRNAs, important clues on general NELF functions may be found in the context of the different mRNA processing steps that are affected by CBC, the first example being histone mRNA 3′ end processing, as we have shown here. Of particular interest, it has been proposed that the participation of CBC in pre-mRNA 3′ end processing is enabled by the communication between the 5′ and 3′ ends of mRNAs due to RNA looping, which apparently can be stabilized by 5′ and 3′ factors. These factors include CBC, CPSF, CstF, RNA, and unidentified intermediates (Flaherty et al., 1997), one of which we think may be NELF. Pushing the idea of collaboration between NELF and CBC even further, we have begun studying potential involvements of NELF in splicing and in RNA export. Thus far, although we have not found significant effects of NELF on splicing using in vitro splicing reactions (data not shown), we have in fact found by using interspecies heterokaryon assays that NELF-E is an actively shuttling protein (T.M.C.Y., T.N., Y.Y., and H.H., unpublished data). As CBC is an essential factor in snRNA nucleocytoplasmic transport (Izaurralde et al., 1995), this immediately leads us to speculate on the potential roles of NELF in the maturation scheme of snRNPs.

Certain parallels can be drawn between histone mRNAs and snRNAs. For example, like histone mRNAs, most snRNAs are RNAPII transcribed, short, intronless, and nonpolyadenylated (Eliceiri and Sayavedra, 1976). What is most significant is that snRNA gene loci are also often clustered and that certain (e.g., U1 and U2 snRNA) genes are associated with CBs (Frey et al., 1999). Since CB/NB pairs that are not associated with histone loci (Figure 6A, red arrow) may be associated with snRNA loci, it will then be interesting to know whether and how NELF may affect snRNA transcription. In this context, it is noteworthy that an RNAPII-associated complex called Integrator (Baillat et al., 2005) was recently identified. This complex consists of at least 12 subunits, including two that are similar to CPSF subunits, and is recruited to the CB-associated U1 and U2 snRNA genes, where it mediates snRNA 3′ end processing. Hence, it will be exciting to find out if there is an snRNA 3′ end processing pathway that is analogous to that of histone 3′ end processing, i.e., through NELF, CBC, and Integrator, thereby extending the general functions of NELF to the processing of another major class of small RNA species in the cell.

EXPERIMENTAL PROCEDURES

Electrophoretic Mobility Shift Assay

pBluescript (Stratagene) was digested with EcoRI and transcribed by T7 RNA polymerase in the presence of [α-^{32}P]-UTP and m^7GpppG. Transcripts (64 nt) were gel purified and then used as the capped RNA probe. Indicated amounts of protein factors and/or HeLa NE and capped RNA probes (~10 fmol) were incubated in 10 μl of buffer containing 20 mM HEPES-NaOH (pH 7.9), 20% glycerol, 100 mM KCl, 0.2 mM EDTA, 10 μg yeast tRNA, 10 μg bovine serum albumin, and 16 units of RNasin (Promega) for 30 min at 30°C. Reactions were analyzed by electrophoresis in 0.5× Tris-borate-EDTA running buffer at 4°C on 4% native polyacrylamide gels, which were then dried and exposed to X-ray films (Kodak).

Knockdown Experiments and DNA Microarray Analysis

shRNA sequences were cloned into pBluescript containing a mouse U6 promoter as described (Yamada et al., 2006). The oligos were annealed and inserted between the BseRI and BglII sites of the plasmid. We constructed the following oligo pairs (sense and antisense strands underlined; italics indicates spacer loop): 5′-ATGGAGTCAGCAGATCAG*TTCAAGAGA*CTGATCTGCTGACTCCATCTTTTT-3′ and 5′-GATCAAAAAGATGGAGTCAGCAGATCAG*TCTCTTGAA*CTGATCTGCTGACTCCATCA-3′ (for NELF-E knockdown), 5′-TGGAATCTGCTCAGAGTG*TTCAAGAGA*CACTCTGAGCAGATTCCACTTTTT-3′ and 5′-GATCAAAAAGTGGAATCTGCTCAGAGTG*TCTCTTGAA*CACTCTGAGCAGATTCCACA-3′ (for CBP80 knockdown), and 5′-TATAGTCGACGTTCATGG*TTCAAGAGA*CCATGAACGTCGACTATACTTTTT-3′ and 5′-GATCAAAAAGTATAGTCGACGTTCATGG*TCTCTTGAA*CCATGAACGTCGACTATACA-3′ (for SLBP knockdown). Then cassettes including the U6 promoter were excised and subcloned into pLenti6 (Invitrogen). Recombinant lentiviruses were produced according to the manufacturer's instructions. In knockdown experiments, HeLa cells were infected with recombinant lentiviruses expressing no shRNA (U6 promoter alone) or expressing shRNA against NELF-E, CBP80, or SLBP and selected in the presence of 4 μg/ml Blasticidin. Five days postinfection, the cells were either lysed with high-salt buffer (50 mM Tris-HCl [pH 7.9], 500 mM NaCl, 1% NP-40, 2 mM EDTA) or harvested for either standard fluorocytometric analysis or RNA preparation for RNase protection assay or DNA microarray analysis. Total RNA was prepared by standard procedures using Sepasol (Nakalai) for RNase protection assays. For microarray analysis, total RNA was prepared using RNeasy Mini kit (Qiagen) and reverse transcribed with T7-oligo(dT), and then biotinylated cRNA was synthesized by one-cycle target labeling reagents (Affymetrix). We used Human Genome Focus Arrays (Affymetrix) representing 8500 genes. For each experimental condition, array data were obtained in triplicate and analyzed by Microarray Suite software (Affymetrix).

3D-FISH Combined with Immunofluorescence Staining

HeLa cells constitutively expressing NELF-A-EYFP were grown on 24 × 60 mm cover slides and synchronized in G1 or S phase by a standard double-thymidine block protocol. The cell-cycle stages were confirmed by FACS analysis. In order to obtain three-dimensionally (3D) preserved cell nuclei, cells were cultured and fixed as described previously (Solovei et al., 2002; Tanabe et al., 2002). For combined IF staining with 3D-FISH procedure, IF of CBs was first performed after the treatment step of five cycles of freeze-thaw in liquid nitrogen. Here, CBs were detected by mouse anti-coilin antibody (BD Biosciences) and Cy3-conjugated sheep anti-mouse secondary antibody (Jackson ImmunoResearch Laboratories). The cover slides were mounted with VectaShield (Vector), and a first round of image capture for NELF-A-EYFP and anti-coilin-Cy3 signals was carried out using a confocal laser scanning microscope (LSM 510 META, Carl Zeiss) equipped with a 63x/1.4 Plan-Apochromat objective. Nuclei were scanned with an axial distance of 200 nm, and light optical section images (512 × 512 pixel resolution) were recorded sequentially for the fluorescent signals from YFP and Cy3. Care was taken to note the exact stage position of each scanned nucleus. In continuation of the 3D-FISH procedure, the cover slides were unmounted after the scanning and incubated in 0.1 N HCl for 10 min, 1% paraformaldehyde in PBS for 10 min, and 50% formamide in 2× SSC for 1 hr. Hybridization was carried out with the DIG-labeled DNA probe for the histone gene cluster at 6p21.3 and a 10-fold excess of human Cot-1 DNA at 37°C for 3 days. The DIG-labeled DNA probe was detected by rabbit anti-digoxygenin antibody (Sigma) and subsequent FITC-conjugated donkey anti-rabbit IgG secondary antibody (Jackson ImmunoResearch Laboratories). The cover slides were counterstained with TOPRO-3 (Molecular Probes) in 2× SSC prior to a second round of image capture for the histone gene cluster on the same nuclei scanned during the first round. Nuclei were scanned under the same conditions as the first round, except that signals from FITC and TOPRO-3 were recorded. The images scanned during the two rounds were combined into one set of image stacks by LSM5 software (Carl Zeiss). 3D reconstruction, in which NBs (yellow), histone loci (green), and Cajal bodies (red) are simultaneously visualized in one nucleus (Figure 6E), was performed by Amira 3.1 TGS software (http://www.amiravis.com/).

Other Experiments

See the Supplemental Experimental Procedures for methods relating to the following: cell lines, recombinant plasmids and proteins, immunoprecipitation, GST pull-down assay, immunoblotting, RNase protection assay, preparation of FISH probes, FISH on metaphase spreads, immunostaining of cleavage bodies, ChIP assay, and quantitative RT-PCR.

Supplemental Data

Supplemental Data include Supplemental Experimental Procedures, Supplemental References, and six figures and can be found with this article online at http://www.molecule.org/cgi/content/full/26/3/349/DC1/.

ACKNOWLEDGMENTS

We thank Iain Mattaj and Rong Li for plasmids and antibodies. We also thank Junko Kato, Tomoko Yamada, Marin Chiba, Taeko Nagata, and Hiroko Awata for expertise and technical support. This work was

supported in part by the Grant of the 21st Century Center of Excellence (COE) Program from the Ministry of Education, Culture, Sports, Science, and Technology (MEXT) and by a grant from the New Energy and Industrial Technology Development Organization (to H.H.). This work was also supported by a Grant-in-Aid for Scientific Research on Priority Areas "Nuclear Dynamics" (to H.T., #17050008) and "DECODE System" (to Y.Y., #17054014) from MEXT and by a grant from the Naito Foundation (to Y.Y.). T.M.C.Y. is supported by a Canadian Institutes of Health Research (CIHR) postdoctoral fellowship.

Received: December 14, 2006
Revised: March 12, 2007
Accepted: April 10, 2007
Published: May 10, 2007

REFERENCES

Aida, M., Chen, Y., Nakajima, K., Yamaguchi, Y., Wada, T., and Handa, H. (2006). Transcriptional pausing caused by NELF plays a dual role in regulating immediate-early expression of the junB gene. Mol. Cell. Biol. *26*, 6094–6104.

Aiyar, S.E., Sun, J.L., Blair, A.L., Moskaluk, C.A., Lu, Y.Z., Ye, Q.N., Yamaguchi, Y., Mukherjee, A., Ren, D.M., Handa, H., and Li, R. (2004). Attenuation of estrogen receptor alpha-mediated transcription through estrogen-stimulated recruitment of a negative elongation factor. Genes Dev. *18*, 2134–2146.

Baillat, D., Hakimi, M.A., Naar, A.M., Shilatifard, A., Cooch, N., and Shiekhattar, R. (2005). Integrator, a multiprotein mediator of small nuclear RNA processing, associates with the C-terminal repeat of RNA polymerase II. Cell *123*, 265–276.

Cioce, M., and Lamond, A.I. (2005). Cajal bodies: a long history of discovery. Annu. Rev. Cell Dev. Biol. *21*, 105–131.

Dominski, Z., Yang, X.C., and Marzluff, W.F. (2005). The polyadenylation factor CPSF-73 is involved in histone-pre-mRNA processing. Cell *123*, 37–48.

Eliceiri, G.L., and Sayavedra, M.S. (1976). Small RNAs in the nucleus and cytoplasm of HeLa cells. Biochem. Biophys. Res. Commun. *72*, 507–512.

Flaherty, S.M., Fortes, P., Izaurralde, E., Mattaj, I.W., and Gilmartin, G.M. (1997). Participation of the nuclear cap binding complex in pre-mRNA 3′ processing. Proc. Natl. Acad. Sci. USA *94*, 11893–11898.

Frey, M.R., and Matera, A.G. (1995). Coiled bodies contain U7 small nuclear RNA and associate with specific DNA sequences in interphase human cells. Proc. Natl. Acad. Sci. USA *92*, 5915–5919.

Frey, M.R., Bailey, A.D., Weiner, A.M., and Matera, A.G. (1999). Association of snRNA genes with coiled bodies is mediated by nascent snRNA transcripts. Curr. Biol. *9*, 126–135.

Fujinaga, K., Irwin, D., Huang, Y., Taube, R., Kurosu, T., and Peterlin, B.M. (2004). Dynamics of human immunodeficiency virus transcription: P-TEFb phosphorylates RD and dissociates negative effectors from the transactivation response element. Mol. Cell. Biol. *24*, 787–795.

Gall, J.G. (2001). A role for Cajal bodies in assembly of the nuclear transcription machinery. FEBS Lett. *498*, 164–167.

Gilmartin, G.M. (2005). Eukaryotic mRNA 3′ processing: a common means to different ends. Genes Dev. *19*, 2517–2521.

Hirose, Y., and Manley, J.L. (2000). RNA polymerase II and the integration of nuclear events. Genes Dev. *14*, 1415–1429.

Izaurralde, E., Lewis, J., McGuigan, C., Jankowska, M., Darzynkiewicz, E., and Mattaj, I.W. (1994). A nuclear cap binding protein complex involved in pre-mRNA splicing. Cell *78*, 657–668.

Izaurralde, E., Lewis, J., Gamberi, C., Jarmolowski, A., McGuigan, C., and Mattaj, I.W. (1995). A cap-binding protein complex mediating U snRNA export. Nature *376*, 709–712.

Lanzotti, D.J., Kaygun, H., Yang, X., Duronio, R.J., and Marzluff, W.F. (2002). Developmental control of histone mRNA and dSLBP synthesis during Drosophila embryogenesis and the role of dSLBP in histone mRNA 3′ end processing in vivo. Mol. Cell. Biol. *22*, 2267–2282.

Li, L., Roy, K., Katyal, S., Sun, X., Bleoo, S., and Godbout, R. (2006). Dynamic nature of cleavage bodies and their spatial relationship to DDX1 bodies, Cajal bodies, and gems. Mol. Biol. Cell *17*, 1126–1140.

Macville, M., Schrock, E., Padilla-Nash, H., Keck, C., Ghadimi, B.M., Zimonjic, D., Popescu, N., and Ried, T. (1999). Comprehensive and definitive molecular cytogenetic characterization of HeLa cells by spectral karyotyping. Cancer Res. *59*, 141–150.

Mandal, S.S., Chu, C., Wada, T., Handa, H., Shatkin, A.J., and Reinberg, D. (2004). Functional interactions of RNA-capping enzyme with factors that positively and negatively regulate promoter escape by RNA polymerase II. Proc. Natl. Acad. Sci. USA *101*, 7572–7577.

Marzluff, W.F. (2005). Metazoan replication-dependent histone mRNAs: a distinct set of RNA polymerase II transcripts. Curr. Opin. Cell Biol. *17*, 274–280.

Matera, A.G. (1999). Nuclear bodies: multifaceted subdomains of the interchromatin space. Trends Cell Biol. *9*, 302–309.

McChesney, P.A., Aiyar, S.E., Lee, O.J., Zaika, A., Moskaluk, C., Li, R., and El-Rifai, W. (2006). Cofactor of BRCA1: a novel transcription factor regulator in upper gastrointestinal adenocarcinomas. Cancer Res. *66*, 1346–1353.

Midorikawa, Y., Tsutsumi, S., Taniguchi, H., Ishii, M., Kobune, Y., Kodama, T., Makuuchi, M., and Aburatani, H. (2002). Identification of genes associated with dedifferentiation of hepatocellular carcinoma with expression profiling analysis. Jpn. J. Cancer Res. *93*, 636–643.

Narita, T., Yamaguchi, Y., Yano, K., Sugimoto, S., Chanarat, S., Wada, T., Kim, D.K., Hasegawa, J., Omori, M., Inukai, N., et al. (2003). Human transcription elongation factor NELF: identification of novel subunits and reconstitution of the functionally active complex. Mol. Cell. Biol. *23*, 1863–1873.

Pei, Y., Schwer, B., and Shuman, S. (2003). Interactions between fission yeast Cdk9, its cyclin partner Pch1, and mRNA capping enzyme Pct1 suggest an elongation checkpoint for mRNA quality control. J. Biol. Chem. *278*, 7180–7188.

Proudfoot, N.J., Furger, A., and Dye, M.J. (2002). Integrating mRNA processing with transcription. Cell *108*, 501–512.

Scharl, E.C., and Steitz, J.A. (1994). The site of 3′ end formation of histone messenger RNA is a fixed distance from the downstream element recognized by the U7 snRNP. EMBO J. *13*, 2432–2440.

Scharl, E.C., and Steitz, J.A. (1996). Length suppression in histone messenger RNA 3′-end maturation: processing defects of insertion mutant premessenger RNAs can be compensated by insertions into the U7 small nuclear RNA. Proc. Natl. Acad. Sci. USA *93*, 14659–14664.

Schul, W., Groenhout, B., Koberna, K., Takagaki, Y., Jenny, A., Manders, E.M., Raska, I., van Driel, R., and de Jong, L. (1996). The RNA 3′ cleavage factors CstF 64 kDa and CPSF 100 kDa are concentrated in nuclear domains closely associated with coiled bodies and newly synthesized RNA. EMBO J. *15*, 2883–2892.

Schul, W., van Der Kraan, I., Matera, A.G., van Driel, R., and de Jong, L. (1999). Nuclear domains enriched in RNA 3′-processing factors associate with coiled bodies and histone genes in a cell cycle-dependent manner. Mol. Biol. Cell *10*, 3815–3824.

Solovei, I., Walter, J., Cremer, M., Habermann, F., Schermelleh, L., and Cremer, T. (2002). FISH on three-dimensionally preserved nuclei. In FISH, A. Practical Approach, B. Beatty, S. Mai, and J. Squire, eds. (Oxford: Oxford University Press), pp. 119–157.

Sullivan, E., Santiago, C., Parker, E.D., Dominski, Z., Yang, X., Lanzotti, D.J., Ingledue, T.C., Marzluff, W.F., and Duronio, R.J. (2001).

Drosophila stem loop binding protein coordinates accumulation of mature histone mRNA with cell cycle progression. Genes Dev. *15*, 173–187.

Tanabe, H., Muller, S., Neusser, M., von Hase, J., Calcagno, E., Cremer, M., Solovei, I., Cremer, C., and Cremer, T. (2002). Evolutionary conservation of chromosome territory arrangements in cell nuclei from higher primates. Proc. Natl. Acad. Sci. USA *99*, 4424–4429.

Tanabe, H., Kupper, K., Ishida, T., Neusser, M., and Mizusawa, H. (2005). Inter- and intra-specific gene-density-correlated radial chromosome territory arrangements are conserved in Old World monkeys. Cytogenet. Genome Res. *108*, 255–261.

Wada, T., Takagi, T., Yamaguchi, Y., Watanabe, D., and Handa, H. (1998). Evidence that P-TEFb alleviates the negative effect of DSIF on RNA polymerase II-dependent transcription in vitro. EMBO J. *17*, 7395–7403.

Wright, T.J., Costa, J.L., Naranjo, C., Francis-West, P., and Altherr, M.R. (1999). Comparative analysis of a novel gene from the Wolf-Hirschhorn/Pitt-Rogers-Danks syndrome critical region. Genomics *59*, 203–212.

Wu, C.H., Yamaguchi, Y., Benjamin, L.R., Horvat-Gordon, M., Washinsky, J., Enerly, E., Larsson, J., Lambertsson, A., Handa, H., and Gilmour, D. (2003). NELF and DSIF cause promoter proximal pausing on the hsp70 promoter in Drosophila. Genes Dev. *17*, 1402–1414.

Xie, S.Q., and Pombo, A. (2006). Distribution of different phosphorylated forms of RNA polymerase II in relation to Cajal and PML bodies in human cells: an ultrastructural study. Histochem. Cell Biol. *125*, 21–31.

Yamada, T., Yamaguchi, Y., Inukai, N., Okamoto, S., Mura, T., and Handa, H. (2006). P-TEFb-mediated phosphorylation of hSpt5 C-terminal repeats is critical for processive transcription elongation. Mol. Cell *21*, 227–237.

Yamaguchi, Y., Takagi, T., Wada, T., Yano, K., Furuya, A., Sugimoto, S., Hasegawa, J., and Handa, H. (1999). NELF, a multisubunit complex containing RD, cooperates with DSIF to repress RNA polymerase II elongation. Cell *97*, 41–51.

Yamaguchi, Y., Filipovska, J., Yano, K., Furuya, A., Inukai, N., Narita, T., Wada, T., Sugimoto, S., Konarska, M.M., and Handa, H. (2001). Stimulation of RNA polymerase II elongation by hepatitis delta antigen. Science *293*, 124–127.

Yamaguchi, Y., Inukai, N., Narita, T., Wada, T., and Handa, H. (2002). Evidence that negative elongation factor represses transcription elongation through binding to a DRB sensitivity-inducing factor/RNA polymerase II complex and RNA. Mol. Cell. Biol. *22*, 2918–2927.

Ye, Q., Hu, Y.F., Zhong, H., Nye, A.C., Belmont, A.S., and Li, R. (2001). BRCA1-induced large-scale chromatin unfolding and allele-specific effects of cancer-predisposing mutations. J. Cell Biol. *155*, 911–921.